High-frequency Induced Voltages on Aboveground Pipelines by Nearby Overhead Transmission Lines

Theofilos A. Papadopoulos, *Senior Member, IEEE*, Zacharias G. Datsios, *Member, IEEE*, Andreas I. Chrysochos, *Member, IEEE*, Amauri G. Martins-Britto, *Member, IEEE*, Pantelis N. Mikropoulos, *Senior Member, IEEE*, and Grigoris K. Papagiannis, *Senior Member, IEEE*

***Abstract*—Lorem ipsum dolor sit amet, consectetuer adipiscing elit. Etiam lobortis facilisis sem. Nullam nec mi et neque pharetra sollicitudin. Praesent imperdiet mi nec ante.**

***Index Terms*—Earth conduction effects, electromagnetic transients, frequency-dependent soil models, overhead lines, pipelines.**

I. Introduction

ELECTROMAGNETIC interference (EMI) between power transmission lines and pipelines sharing the same right-of-ways has been a topic of major concern for several decades now. this has been intensified by the increasing industrialization, the more restrictive environmental regulations and the ever-increasing cost of rights-of-ways [1], [2], [3]. In general, EMI pertains to the act of three coupling mechanisms, namely the inductive (or electromagnetic), the capacitive (or electrostatic), and the conductive (or resistive) [3], [4].

Therefore, in the presence of a neighboring pipeline, potentially hazardous voltages may be transferred to the victim circuit. Consequently, a significant issue is to keep the voltage in all metallic parts within acceptable limits, since induced overvoltages may result in (a) safety hazards, due to electric shock to people coming in contact, (b) pipeline aging and insulation failures that subsequently can contribute to pipeline corrosion, and (c) damages to the equipment and devices connected to the cables and the pipeline [3], [5], [6].

It is, thus, imperative to assess the induced voltages on pipelines caused by overhead transmission lines (OHLs). Most of these studies refer to cases during the normal operating condition or during faults at the mains frequency (50 Hz or 60 Hz). Recently, a few works have presented preliminary EMI results at higher frequencies, e.g., by investigating harmonic induction effects [7], [8] and the impact of transient surges on pipelines [2], [5], [6], [9], [10]. This is becoming more important for aboveground pipelines, where induced voltages from lightning and/or switching events are significant in comparison to power frequency faults [5], [6]. All these studies to predict the effects of transient EMI are based on electromagnetic transient (EMT) models and require the calculation of the per-unit-length self and mutual parameters (impedances and admittances) between the OHL and the pipeline. For their accurate estimation the influence of the imperfect earth is a crucial issue. For overhead conductors the most known formulation has been proposed by Carson [11]. However, Carson's work is based on a series of assumptions regarding earth conduction effects; of those the most important are [12]:

- The influence of the imperfect earth is considered only on the conductor impedance, neglecting admittance earth conduction effects. This implies that earth behaves only as a conductor limiting the accuracy of such an approach to low-frequency applications, e.g., up to a few kHz. Many efforts to develop expressions for the series impedances have been reported in literature, with the most known proposed by Sunde, that extends [8] by including earth permittivity.
- The frequency-dependent (FD) electrical properties of soil [13], [14], [15], [16], [17], i.e., conductivity and permittivity, are assumed to be constant (CP).

In order to develop more accurate earth models in the high frequency (HF) region, Wise [18], [19] introduced a different earth approach aiming at the calculation of the earth conduction effects on both the series impedance and the shunt admittance. Respectively, Kikuchi [20] by investigating the transition from quasi-TEM to surface wave guide propagation proposed also earth impedance and admittance formulas which under specific approximations result to those found by Wise. Later, Pettersson [21] approximated Kikuchi's and Wise's infinite integral expressions with logarithmic terms, providing an easily feasible formulation [22]. These approaches have been used to investigate the transient performance of OHLs [22], [23], [24] as well as gas insulated buses [25]; however, they have not been applied to EMI problems. Additionally, several models have been proposed for the prediction of the FD soil electrical properties [13], [14], [16], [15], [17]. The effects of the application of these models have attracted much attention recently. However, most studies focus on OHL configurations [17], [26], [27], [28] and underground cable systems [29], [30], [31]. Therefore, the impact of earth conduction effects at HFs on configurations incorporating OHLs and pipelines has not been addressed in the literature.

This paper investigates the effect of the frequency-

Theofilos A. Papadopoulos is with Power Systems Laboratory,Department of Electrical and Computer Engineering, Democritus University of Thrace, 67100 Xanthi, Greece (e-mail: thpapad@ee.duth.gr).

Zacharias G. Datsios, Pantelis N. Mikropoulos, and Grigoris K. Papagiannis are with the School of Electrical and Computer Engineering, Aristotle University of Thessaloniki, 54124 Thessaloniki, Greece (e-mail: zdatsios@auth.gr; pnm@eng.auth.gr; grigoris@eng.auth.gr).

Andreas I. Chrysochos is with Cablel Hellenic Cables S.A., Maroussi, 15125 Athens, Greece (e-mail: achrysochos@fulgor.vionet.gr).

Manuscript received March 31, 2022.

dependence of the soil electrical properties on high frequency induced voltages on aboveground pipelines subjected to disturbances caused by nearby OHLs. To carry out this task, the propagation characteristics of an OHL-pipeline configuration are calculated by using Wise's earth formulation taking into account earth conduction effects on both the series impedances and shunt admittances. CP and FD soil models are employed in the calculation of the propagation characteristics of the configuration. Results are also compared and discussed on the basis of frequency-domain and EM induced voltage responses at the pipeline.

II. Mathematical Model

A. Earth impedance and admittance formulas

Let us assume the case of two thin wires situated in the topology of Fig. 1. Wise's generalized formulas, representing the influence of the conductive and displacement currents in all propagation media on the per-unit-length earth impedance ($Z_{e_{ij}}$) and earth admittance (Y_{e_i}) is given as (1)-(5) in integral form.

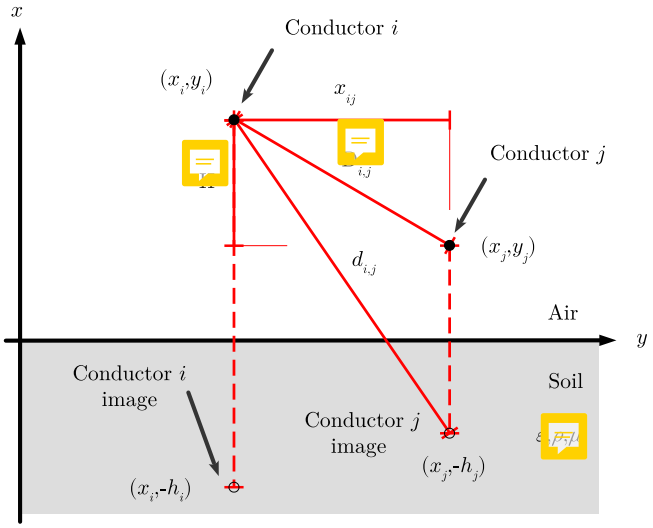

Fig. 1. Two parallel thin conductors above earth surface.

$$Z_{\varepsilon_j} = \frac{j\omega\mu_0}{2\pi}\left(\ln\frac{D_{ij}}{d_{ij}} + M_{ij}\right), \tag{1}$$

$$Y_{\varepsilon_{ij}} = j\omega P_{e_{ij}}^{-1} = j\omega P_{pg_{ij}} + P_{g_{ij}}^{-1}, \tag{2}$$

$$\begin{aligned} M_{ij} &= \int_0^\infty \frac{2\mu_g e^{-h_i+h_i,a_0}}{a_g\mu_0 + a_0\mu_g}\cos(x_{ij}\lambda)d\lambda \\ &\approx \ln\frac{\sqrt{\left(h_i+h_j+\frac{2}{\sqrt{\gamma_g^2-\gamma_0^2}}\right)^2 + x_{ij}^2}}{D_{ij}}, \end{aligned} \tag{3}$$

$$P_{e_i} = P_{P_{g_j}} + P_{8_j} = \frac{1}{2\pi\varepsilon_0}\left(\ln\frac{D_{ij}}{d_{ij}} + Q_{ij}\right), \tag{4}$$

$$\begin{aligned} Q_{ij} &= \int_0^\infty \frac{2\mu_g\gamma_0^2\mu_0\alpha_0 + \alpha_g\mu_g e^{-h_i+h_i}a_0}{a_g\mu_0 + a_0\mu_g\left(a_g\gamma_0^2\mu_g + a_0\gamma_g^2\mu_0\right)}\cos(x_{ij}\lambda)d\lambda \\ &\approx \frac{1}{(n^2+1)\pi\varepsilon_0}\ln\frac{\sqrt{h_i+h_j+\frac{n^2+1}{\sqrt{\gamma_8^2-\gamma_0^2}}+x_{ij}^2}}{D_{ij}}, \end{aligned} \tag{5}$$

in which λ is the integration variable, $Z_{pg_{ij}}$,$P_{pg_{ij}}$ represent the influence of the perfectly conducting earth and $Z_{g_{ij}}$,$P_{g_{ij}}$ represent the influence of the imperfect earth, respectively. The electromagnetic (EM) properties of air, i.e., permittivity, permeability and conductivity are denoted as ϵ_0, μ_0, (σ_0) and of earth $\epsilon_g = \epsilon_{rg}\epsilon_0$, $\mu_g = \mu_{rg}\mu_0$, σ_g; ϵ_{rg} is the relative permittivity and μ_{rg} the relative permeability of the earth. Accordingly, the air and earth propagation constants are defined as $\gamma_0 = jk_0 = j\omega\sqrt{\mu_0\varepsilon_0}$ and $\gamma_g = \sqrt{j\omega_0\left(\sigma_g + j\omega\varepsilon_0\varepsilon_{r_g}\right)}$, respectively, and $a_0 = \lambda$ and $a_g = \sqrt{\lambda^2+\gamma_g^2+k_0^2}$; $D_{ij} = \sqrt{H^2+(x_i-x_j)^2}$, $d_{ij} = \sqrt{(h_i-h_j)^2+(x_i-x_j)^2}$. The self impedance of conductor i is derived by replacing h_j with h_i and x_{ij} with the conductor outer radius r_i. In addition, by numerically approximating the integrals of (3) and (5) with logarithmic terms, Pettersson's simplified expressions are derived with $n = \sqrt{\varepsilon_{r_g} + \frac{\sigma_g}{j\omega\varepsilon_0}}$.

In the case of an OHL and an aboveground pipeline configuration, the total per-unit-length impedance and admittance matrices are derived by applying the generalized formulation of [30]. Apart form the self and mutual earth impedance and earth admittance, the skin effect on the conductor self-impedance is also taken into account and the insulation of the pipeline is expressed in the corresponding self-inductance and -capacitance.

B. Soil modelling

The macroscopic EM behavior of soil is determined by its multiphase particulate nature, that is, by the interaction of its constituents and their individual properties. Regarding EM problems, the behavior of soil (dispersive lossy dielectric material) can be described via two quantities: the relative permittivity, ε_g, and the conductivity, σ_g. These quantities are FD due to dynamic polarization processes as opposed by inertia. The exact value of DC conductivity is also required for a complete EM characterization so as to discern between the contribution of polarization and conduction losses; however, this is not necessary for dealing with EM problems. A more detailed account on the EM behavior of soil has been given in [14].

The electrical properties of soil (ε_{rg}, σ_g) can be predicted using models appropriate for engineering applications; these models describe the variation of ε_{rg} and σ_{rg} with excitation frequency. Several FD soil models applicable to the switching and lightning transients frequency range have been proposed in literature [12], [15]. In this paper, the Longmire and Smith (LS) [13]] and the CIGRE WG C4.33 [3] soil models were adopted based on the discussion of [12]. The former model is based on laboratory measurements (f: 100 Hz – 200 MHz) and

was verified through circuit analysis. The latter was derived on the basis of field tests (f: 100 Hz – 4 MHz).

According to the LS soil model, ε_{rg} and σ_{rg} (S/m) are estimated as [13]

$$\varepsilon_{rg}(f) = \varepsilon_{rg,\infty} + \sum_{n=1}^{13} \frac{a_n}{1+(f/f_n)^2} \tag{6}$$

$$\sigma_g(f) = \sigma_{g,DC} + 2\pi f \varepsilon_0 \sum_{n=1}^{13} \frac{a_n f/f_n}{1+(f/\mathrm{f_n})^2} \tag{7}$$

where f (Hz) is the frequency, ($\varepsilon_{rg,\infty}$ is the HF relative permittivity of soil (equal to 5 according to [13]), a_n (p.u.) are empirical coefficients given in Table 1 of [13], and f_n (Hz) are scaling coefficients [15] calculated as a function of the DC soil conductivity, $\sigma_{g,DC}$ (S/m).

$$f_n = 10^{n-1}(125\sigma_{g,DC})^{0.8312}. \tag{8}$$

The corresponding ε_{rg} and σ_{rg} (S/m) expressions for the CIGRE model are [17]

$$\varepsilon_{rg}(f) = 12 + 9.5 \cdot 10^4 \sigma_{g,LF}^{0.27} f^{-0.46} \tag{9}$$

$$\sigma_g(f) = \sigma_{g,LF} + 4.7 \cdot 10^{-6} \sigma_{g,LF}^{0.27} f^{0.54} \tag{10}$$

where $\sigma_{g,LF}$ (S/m) is the soil conductivity at 100 Hz.

It is noted that, according to common practice, the low-frequency (LF) soil conductivity $\sigma_{g,LF}$ (typically at 100 Hz) and the HF relative permittivity $\varepsilon_{rg,\infty}$ (1 MHz or higher) are used where frequency-independent (constant) soil electrical properties are adopted. In this study, nine soil cases are investigated: (a) three CP cases (σ_{rg}, ε_{rg}): (0.01 S/m, 15), (0.001 S/m, 5), and ($2 \cdot 10^{-4}$ S/m, 3), (b) three FD cases adopting the LS soil model [13] and (c) three FD cases adopting the CIGRE soil model [17]. For the six FD cases: $\sigma_{rg,100Hz}$ = 0.01, 0.001 and $2 \cdot 10^{-4}$ S/m. The investigated LF conductivity values correspond to soil resistivities of 100, 1000, and 5000 Ωm, covering a wide range of soils commonly found in real world installations [32].

C. System configuration

Fig. 2 shows the cross-section view of the investigated configuration, which comprises of an OHL sharing the same right-of-way with an aboveground pipeline. More specifically, the interfering system is an 150 kV single-circuit OHL with phase conductors in flat formation and two ground wires. The interfered system is a metallic gas/oil coated pipeline installed at a height of 1 m above ground at a horizontal distance of 10 m from the OHL. Fig. 2 depicts the cross-section and EM properties of the pipeline. It is noted that the latter has been used in EMI investigations before [].

III. Propagation Characteristics

In this section, the propagation characteristics of a system composed of an OHL in close proximity with an aboveground metallic pipeline are investigated in detail. The different propagation modes, characteristic impedances, attenuation constants and phase velocities are analyzed in the frequency-domain using different formulations and soil models, with emphasis on the modes which are most affected by earth properties.

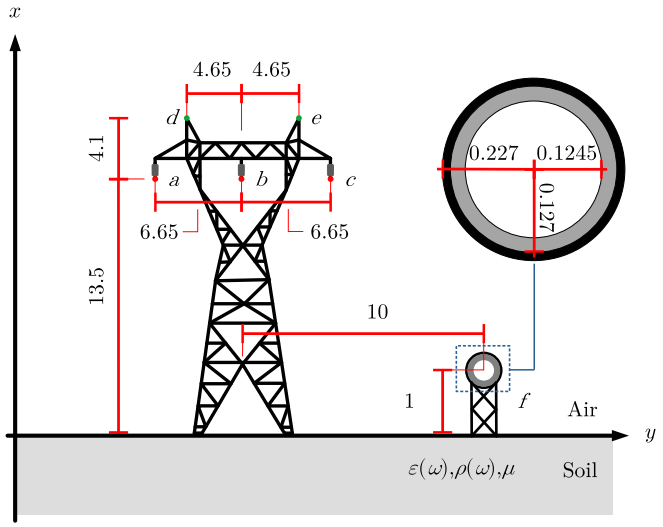

Fig. 2. Cross-section view of the system under investigation.

A. Modal analysis

The attenuation and velocity characteristics of the six natural modes of wave propagation are shown in Fig. 4a and 4b, respectively, by adopting Wise's formula and constant soil properties with soil resistivity equal to $1000\Omega m$. However, the analysis below is similar with respect to any other formulation for per-unit-length parameters and soil. Modes #1 and #2 are mainly associated with ground wires. Mode #1 is energized by injecting a unit current into the ground wire d and extracting it from ground wire e. Mode #2 is energized by injecting a unit current into both ground wires and extracting it by the three phases a, b and c. These 2 modes have a quasi-constant attenuation over a wide frequency band, while their velocities approach the speed of light at high frequency. Mode #3 is a ground mode, having the characteristics of relatively high attenuation and very low velocity. The latter is due to the high inductive impedance of the soil path and increases only slowly with frequency. Mode #4 is associated with the remote metallic pipeline. This mode is energized by injecting a unit current into the pipeline and extracting it from the phases and the ground wires. This mode is characterized by high attenuation and high velocity, with the latter being also influenced by the dielectric medium. Modes #5 and #6 are low-attenuation interphase modes with velocities approaching the speed of light at high frequency. Mode # 5 is energized by injecting a unit current through phase a and extracting it through phase c. On the other hand, Mode #6 is energized by injecting two units of

current through phase b and extracting half of this from phase a and the other half from phase c.

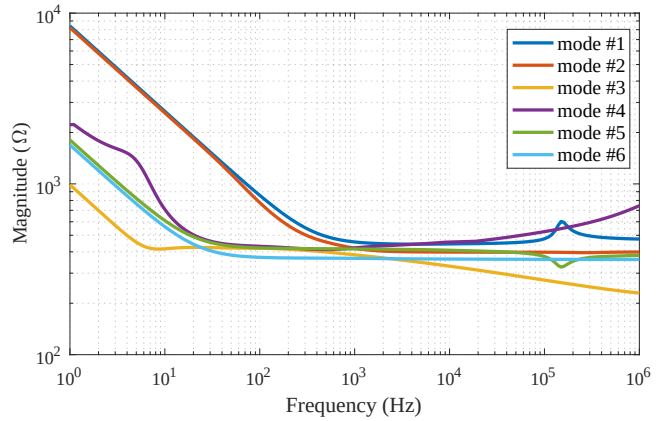

Fig. 3. Characteristic impedance magnitude (a) and angle (b), Wise's formula, constant soil properties with $\rho = 1000\ \Omega m$.

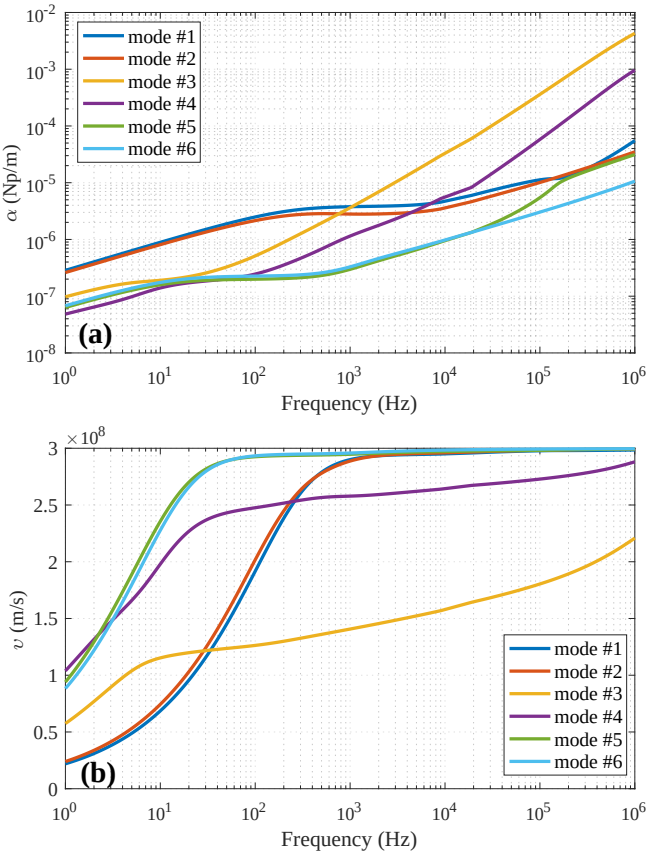

Fig. 4. Attenuation constant (a) and phase velocity (b), Wise's formula, constant soil properties with $\rho = 1000\ \Omega m$.

B. Influence of earth admittance correction

The influence of earth impedance and admittance correction terms is assessed by comparing results obtained using Wise's formulas expressed in (3) and (5) to the classic Carson's equation, under which the soil permittivity is disregarded [11].

Soil properties are assumed to be constant, and different resistivity values are employed, namely: 100 Ωm, 1000 Ωm, and 5000 Ωm, covering a wide range of soils commonly found in real world installations [32]. Attenuation constants and phase velocities are evaluated accordingly, and to highlight the differences between each approach, normalized parameters are provided as the ratio with respect to Carson's results:

$$f_{norm} = \frac{\text{propagation characteristics}_{\text{ Wise}}}{\text{propagation characteristics}_{\text{ Carson}}}, \qquad (11)$$

in which f_{norm} denotes the normalized propagation parameter of interest: attenuation constant or phase velocity, in p.u.

The propagation characteristics for mode #3 (pure ground mode) are represented in Figs. 6 and 7, whereas results for mode #4 (pipeline mode) are given in Figs. 8 and 9.

In general, ground mode waves attenuate more steeply and propagate slower than the pipeline (aerial) mode, which agrees with the finite earth resistivity yielding a lossy medium, in contrast to the insulating air within which the pipeline is installed.

Results are essentially the same at the lower part of the frequency spectrum, however, after 10 kHz, discrepancies become more pronounced in Wise's model for increasing resistivity values. The influences of the soil resistivity in the propagation characteristics determined using Carson's formula are nearly negligible, which not only agrees with previous reports in the literature [29], but it is also algebraically consistent with the potential coefficient definition in (4). Under Carson's model and electrostatic images theory, the term Q_{ij} in (4) equals to zero, nullifying the effect of imperfect earth on line admittances and, consequently, on propagation characteristics.

On the other hand, Wise's formulation curves provide a clear perspective of how the earth admittance correction affects the attenuation constants and phase velocities of propagating waves, which is particularly evident from inspection of the normalized values for $\rho = 5000\ \Omega m$. It can be seen that, in the worst case, Wise's attenuation constant more than doubles in relation to Carson's result, which corresponds to a discrepancy of over 100%. Similarly, phase velocities are increased when earth return admittances are accounted for, with discrepancies of around 5% (pipeline mode) to 30% (ground mode).

It can be generally concluded from above that neglecting earth return correction on line admittances may disregard important propagation effects taking place both on the interfering as well as the interfered installation, leading to innacurate induced voltage predictions, especially at higher frequencies, as demonstrated in Section IV.

C. Influence of soil model

To evaluate the influence of the soil properties frequency-dependence on propagation characteristics, results obtained employing Wise's formula along with the Longmire-Smith (LS) and CIGRE models are compared to the constant properties (CP) model by means of normalized curves, taking the CP model as reference. Figs. 10 and 11 describe the normalized propagation parameters for ground mode and pipeline mode waves, respectively, considering different LF resistivity values of 100 Ωm, 1000 Ωm and 5000 Ωm.

As in the preceding section, the largest discrepancies occur for ground mode waves within the upper portion of the frequency spectrum and higher soil resistivities. In general, curves for both LS and CIGRE models show the same trend, but with slightly increased influence for the CIGRE model, mainly due to the considerably lower resistivity values predicted for higher resistivity soils by this soil model. In particular, as seen from Figs. 10 and 11, the lowest deviations (up to 5%) are observed for the highly conductive soil of $100\ \Omega m$. For this case, relative permittivity effects, as well as the effects of the reduction of resistivity with increasing frequency ($\rho_{1,MHz} \approx 0.8\rho_{100Hz}$) on propagation characteristics are minimal. For the other two soil cases of $1000\ \Omega m$ and $5000\ \Omega m$, significant differences are observed for the attenuation constant; this also applies for the ground mode velocity of the $5000\ \Omega m$ soil at higher frequencies. These are attributed to the notable decrease of soil resistivity with increasing frequency (CIGRE soil model: $\rho_{1,MHz} \approx 0.45\rho_{100Hz}$ and $\rho_{1,MHz} \approx 0.2\rho_{100Hz}$ for the $1000\ \Omega m$ and $5000\ \Omega m$, respectively), combined with the increased influence of permittivity with frequency. For higher resistivity soils, these effects become more pronounced at lower frequencies, and hence, for such soils the frequency-dependence of soil properties should be taken into account.

IV. Pipeline induced voltages

To demonstrate the effect of soil modelling on induced pipeline voltages, frequency-domain (FD) and time-domain (TD) calculations are performed by applying a voltage source at the sending end of conductor *a* of Fig. 2. Characteristic impedance terminations are applied to the OHL (remaining conductors and skywire) and pipeline ends. To determine the characteristic impedances calculations have been carried out considering the single conductor case, i.e., phase conductor, skywire and pipeline, resulting into values of 574 Ω, 1354 Ω and 306 Ω, respectively. Therefore, the OHL and the pipeline approximately extend beyond the parallelism without earthing; thus the effect of conductive coupling can be neglected. For both FD and TD anlysis, the simulation model of [33] is used assuming varying OHL/pipeline parallelism length, i.e., ℓ=100 m, 1000 m, and 10000 m and soil resistivity, i.e., $\rho_{1,LF}$ = $100\ \Omega m$, $1000\ \Omega m$ and $5000\ \Omega m$.

A. Frequency-domain responses

A 1-V rms source is injecting sinusoidal signals in the frequency range of 1 kHz to 1 MHz. In Fig. xx the induced voltage spectrum at the pipeline receiving end is summarized for all examined cases of soil resistivity and parallelism. The FD responses are simulated following Carson's and Wises's approaches. For both earth approaches the soil properties are taken constant and frequency dependent according to the LS and the CG soil models.

Subjected to inductive and capacitive coupling the maximum induced voltage of the pipeline appears at its ends [6]. In Fig. xx the induced voltage spectrum at the pipeline receiving end is plotted. Spectrum peaks and notches are observed [5], [6] because the OHL and the pipeline are nearly matched. Perfect matching for multiconductor configurations and subsequently a flat voltage spectrum requires the termination of the configuration ends via a FD complex impedance matrix [34]. The induced voltage spectrum and particularly the spectrum peaks gradually increase with the soil resistivity and parallelism length, due to the increasing effect of predominant inductive coupling between the OHL and the pipeline. Comparing the spectra of the different cases deviations are observed. This is more pronounced for poorly conductive soils and for short lengths of parallelism, since the frequency spectrum shifts gradually to higher frequencies where the impact of earth admittance and soil dispersion are more significant. This can be realized by $f = \upsilon/\ell$, where υ is the wave propagation and ℓ the parallelism length [12], [22]. As Wise's formulation takes into account the earth admittance in the pipeline parameters, the obtained voltage spectra present a lower amplitude. Regarding the effect of soil models deviations with the CP soil case are higher for the CG model at $\rho_{1,LF}$=100 Ωm. However, for higher soil resistivity, differences are more marked with the LS model instead of the CG. This can be substantiated by the variation of the soil electrical properties against frequency as discussed in Section xx.

B. Transient responses

To demonstrate the effect of Wise's models on transient responses, a voltage source producing a 1.2/50 μs double-exponential waveform of 1 pu amplitude is applied to the sending end of the OHL conductor #a at $t = 0s$. The transient responses are presented in Fig. xx for $\rho_{1,LF}$=1000 Ωm and parallelism length 1 km. In the same figures transient results obtained with Carson's earth formulation are also compared. Also the transient responses simulations reveal the effect of the adopted earth formulation and soil model on the transient responses. This is more evident at the induced voltage peak, which is determined by the high frequency dominant frequency (see Fig. xx) [35].

Wise's transient responses are also compared with the approximate Petttersson's earth formulation. In Fig. xx the absolute deviation is depicted for the different soil cases; the parallelism length is 1 km. The comparison leads to small deviations, which generally increase with the soil resistivity but not exceeding 2.5 % (induced peak voltage). These results justify the use of the approximate yet accurate Petttersson's model for investigating high frequency phenomena up to some MHz; this is in consistency with the findings of [24].

V. Conclusions

Lorem ipsum dolor sit amet, consectetuer adipiscing elit. Etiam lobortis facilisis sem. Nullam nec mi et neque pharetra sollicitudin. Praesent imperdiet mi nec ante.

Acknowledgments

Lorem ipsum dolor sit amet, consectetuer adipiscing elit. Etiam lobortis facilisis sem. Nullam nec mi et neque pharetra sollicitudin. Praesent imperdiet mi nec ante.

REFERENCES

[1] G. C. Christoforidis, D. P. Labridis, and P. S. Dokopoulos, "Inductive interference on pipelines buried in multilayer soil due to magnetic fields from nearby faulted power lines," *IEEE Trans. Power Del.*, vol. 47, no. 2, pp. 254–262, 2005.

[2] A. G. Martins-Britto, C. M. Moraes, and F. V. Lopes, "Transient electromagnetic interferences between a power line and a pipeline due to a lightning discharge: An emtp-based approach," *Electric Power Systems Research*, vol. 197, p. 107321, 2021.

[3] CIGRE, "Guide concerning influence of high voltage ac power systems on metallic pipelines," *CIGRE Working Group 36.02*, 1995.

[4] F. P. Dawalibi and R. D. Southey, "Analysis of electrical interference from power lines to gas pipelines. i. computation methods," *IEEE Trans. Power Del.*, vol. 4, no. 3, pp. 1840–1846, 1989.

[5] I. Cotton, K. Kopsidas, and Y. Zhang, "Comparison of transient and power frequency-induced voltages on a pipeline parallel to an overhead transmission line," *IEEE Trans. Power Del.*, vol. 22, no. 3, pp. 1706–1714, 2007.

[6] K. Kopsidas and I. Cotton, "Induced voltages on long aerial and buried pipelines due to transmission line transients," *IEEE Trans. Power Del.*, vol. 23, no. 3, pp. 1535–1543, 2008.

[7] D. Boteler, C. A. Charalambous, and K. Lax, "New insights into calculations of ac interference at fundamental and harmonic frequencies taking account of the phase relationships of the currents," *IEEE Trans. Power Del.*, 2021.

[8] J. Yong, B. Xia, H. Yong, W. Xu, A. B. Nassif, and T. C. Hartman, "Harmonic voltage induction on pipelines: Measurement results and methods of assessment," *IEEE Trans. Power Del.*, vol. 33, no. 5, pp. 2170–2179, 2018.

[9] G. D. Peppas, M. P. Papagiannis, S. Koulouridis, and E. C. Pyrgioti, "Induced voltage on a above-ground natural gas/oil pipeline due to lightning strike on a transmission line," in *2014 International Conference on Lightning Protection (ICLP)*, 2014, pp. 461–467.

[10] D. Caulker, H. Ahmad, and M. S. M. Ali, "Effect of lightning induced voltages on gas pipelines using atp-emtp program," in *2008 IEEE 2nd International Power and Energy Conference*, 2008, pp. 393–398.

[11] J. Carson, "Wave propagation in overhead wires with ground return," *Bell Syst. Tech. J.*, p. 539–554, 1926.

[12] T. A. Papadopoulos, Z. G. Datsios, A. I. Chrysochos, P. N. Mikropoulos, and G. K. Papagiannis, "Wave Propagation Characteristics and Electromagnetic Transient Analysis of Underground Cable Systems Considering Frequency-Dependent Soil Properties," *IEEE Transactions on Electromagnetic Compatibility*, vol. 63, no. 1, pp. 259–267, 2021.

[13] C. Longmire and K. Smith, "A universal impedance for soils," *DNA 3788T, Mission Research Corp., Santa Barbara, CA*, 1975.

[14] R. Alipio and S. Visacro, "Modeling the frequency dependence of electrical parameters of soil," *IEEE Transactions on Electromagnetic Compatibility*, vol. 56, no. 5, pp. 1163–1171, 2014.

[15] D. Cavka, N. Mora, and F. Rachidi, "A comparison of frequency-dependent soil models: Application to the analysis of grounding systems," *IEEE Transactions on Electromagnetic Compatibility*, vol. 56, no. 1, pp. 177–187, 2014.

[16] Z. G. Datsios and P. N. Mikropoulos, "Characterization of the frequency dependence of the electrical properties of sandy soil with variable grain size and water content," *IEEE Transactions on Dielectrics and Electrical Insulation*, vol. 26, no. 3, pp. 904–912, 2019.

[17] CIGRE, "Impact of soil-parameter frequency dependence on the response of grounding electrodes and on the lightning performance of electrical systems," *CIGRE WG C4.33*, 2019.

[18] W. Wise, "Propagation of high frequency currents in ground return circuits," *Proc. Inst. Radio Eng.*, vol. 22, p. 522–527, 1934.

[19] ——, "Potential coefficients for ground return circuits," *Bell Syst. Tech. J.*, vol. 27, p. 365–371, 1948.

[20] H. Kikuchi, "Wave propagation along an infinite wire above ground at high frequencies," *Electrotech. J. Jpn.*, vol. 2, p. 73–78, 1956.

[21] P. Pettersson, "Image representation of wave propagation on wires above, on and under ground," *IEEE Transactions on Power Delivery*, vol. 9, no. 2, pp. 1049–1055, 1994.

[22] T. Papadopoulos, A. Chrysochos, C. Traianos, and G. Papagiannis, "Closed-form expressions for the analysis of wave propagation in overhead distribution lines," *Energies*, vol. 13, p. 4519, 2020.

[23] M. D'Amore and M. Sarto, "Simulation models of a dissipative transmission line above a lossy ground for a wide-frequency range. i. single conductor configuration," *IEEE Transactions on Electromagnetic Compatibility*, vol. 38, no. 2, pp. 127–138, 1996.

[24] T. Papadopoulos, G. Papagiannis, and D. Labridis, "A generalized model for the calculation of the impedances and admittances of overhead power lines above stratified earth," *Electr. Power Syst. Res.*, vol. 80, p. 1160–1170, 2010.

[25] A. Ametani, Y. Miyamoto, Y. Baba, and N. Nagaoka, "Wave propagation on an overhead multiconductor in a high-frequency region," *IEEE Transactions on Electromagnetic Compatibility*, vol. 56, no. 6, pp. 1638–1648, 2014.

[26] A. C. S. de Lima and C. Portela, "Inclusion of frequency-dependent soil parameters in transmission-line modeling," *IEEE Transactions on Power Delivery*, vol. 22, no. 1, pp. 492–499, 2007.

[27] M. Tomasevich, Y. Mashenko, and A. C. S. Lima, "Impact of frequency-dependent soil parameters in the numerical stability of image approximation-based line models," *IEEE Transactions on Electromagnetic Compatibility*, vol. 58, no. 1, pp. 323–326, 2016.

[28] M. A. O. Schroeder, M. T. C. de Barros, A. C. S. Lima, M. M. Afonso, and R. A. R. Moura, "Evaluation of the impact of different frequency dependent soil models on lightning overvoltages," *Electr. Power Syst. Res.*, vol. 159, p. 40–49, 2018.

[29] T. Papadopoulos, Z. Datsios, A. Chrysochos, P. Mikropoulos, and G. Papagiannis, "Modal propagation characteristics and transient analysis of multiconductor cable systems buried in lossy dispersive soils," *Electr. Power Syst. Res.*, vol. 196, p. 107249, 2021.

[30] A. Ametani, "A general formulation of impedance and admittance of cables," *IEEE Transactions on Power Apparatus and Systems*, vol. PAS-99, no. 3, pp. 902–910, 1980.

[31] H. Xue, A. Ametani, Y. Liu, and J. De Silva, "Effect of frequency-dependent soil parameters on wave propagation and transient behaviors of underground cables," *Int. J. Electr. Power Energy Syst.*, vol. 122, p. 106163, 2020.

[32] J. He, R. Zeng, and B. Zhang, *Methodology and Technology for Power System Grounding*. Singapore: John Wiley & Sons Singapore Pte. Ltd., 2013.

[33] A. Chrysochos, T. Papadopoulos, and G. Papagiannis, "Enhancing the frequency-domain calculation of transients in multiconductor power transmission lines," *Electric Power Systems Research*, vol. 122, pp. 56–64, 2015.

[34] J. Knockaert and J. P. J. C. R. Belmans, "General equations for the characteristic impedance matrix and termination network of multiconductor transmission lines," in *2009 IEEE International Conference on Industrial Technology*, 2009, pp. 1–6.

[35] A. I. Chrysochos, T. A. Papadopoulos, and G. K. Papagiannis, "Rigorous calculation method for resonance frequencies in transmission line responses," *IET Generation, Transmission Distribution*, vol. 9, pp. 767–778(11), May 2015.

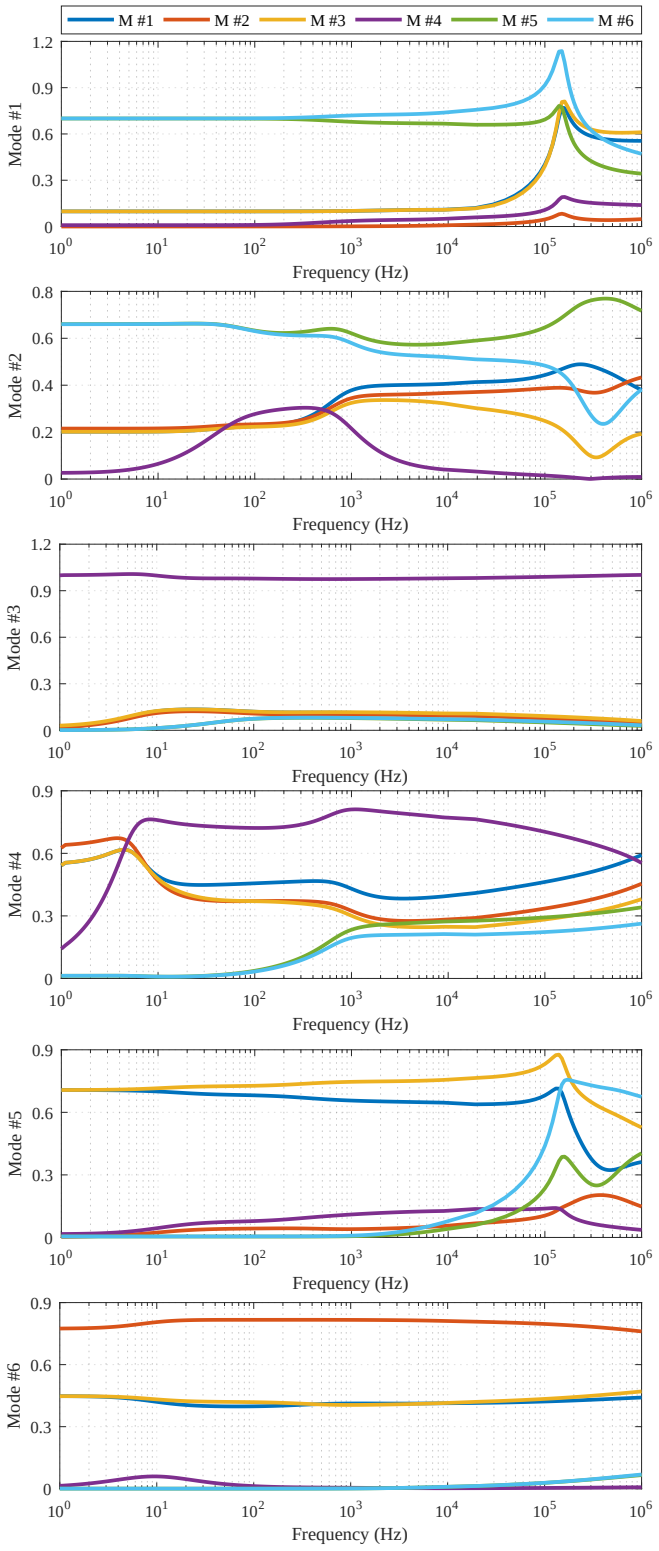

Fig. 5. Modal transformation matrix magnitude considering Wise's formula, constant soil properties with $\rho = 1000\ \Omega m$.

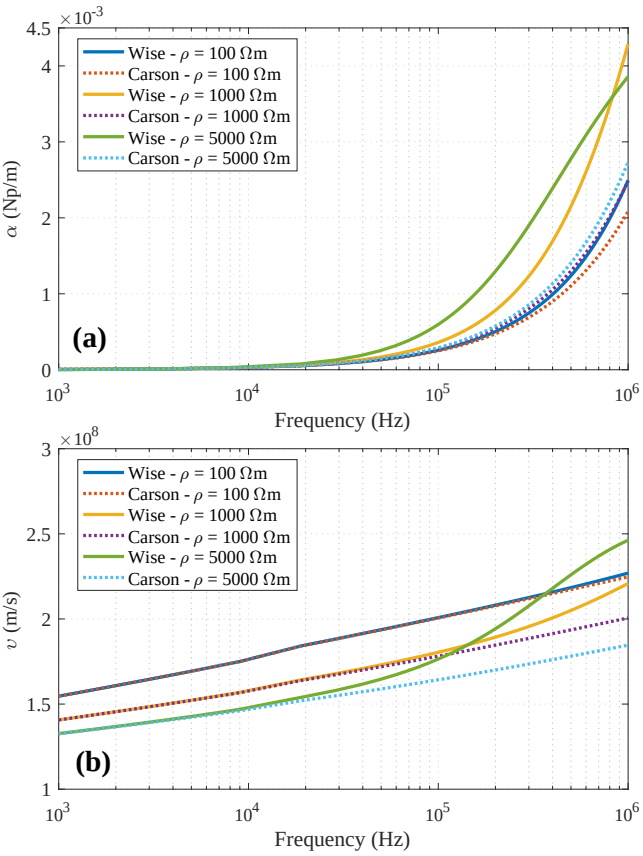

Fig. 6. Attenuation constant (a) and phase velocity (b) for mode #3 (ground mode), comparing Carson and Wise's admittance formulas, with constant soil properties and different soil resistivities.

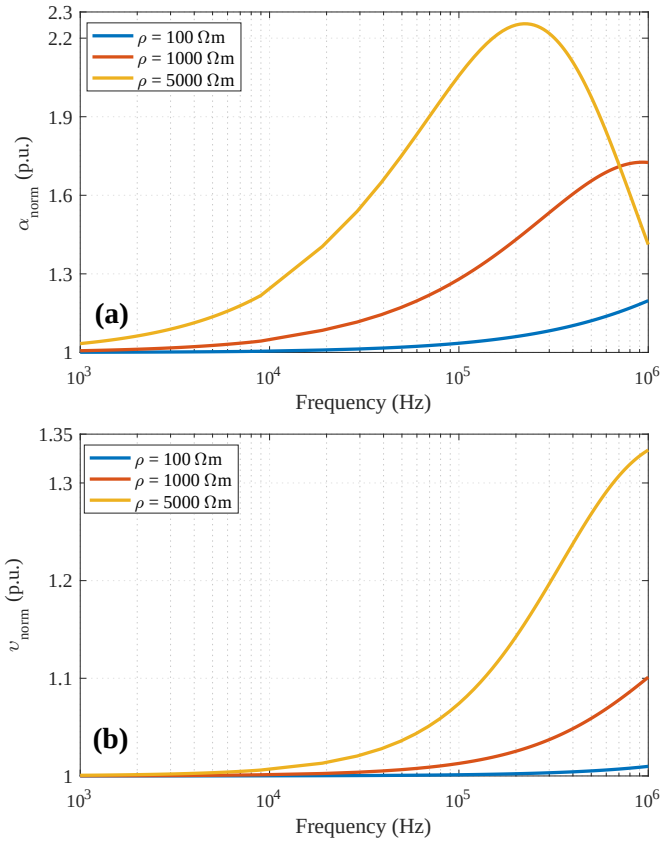

Fig. 7. Normalized attenuation constant (a) and phase velocity (b) for mode #3 (ground mode), comparing Carson and Wise's admittance formulas, with constant soil properties and different soil resistivities.

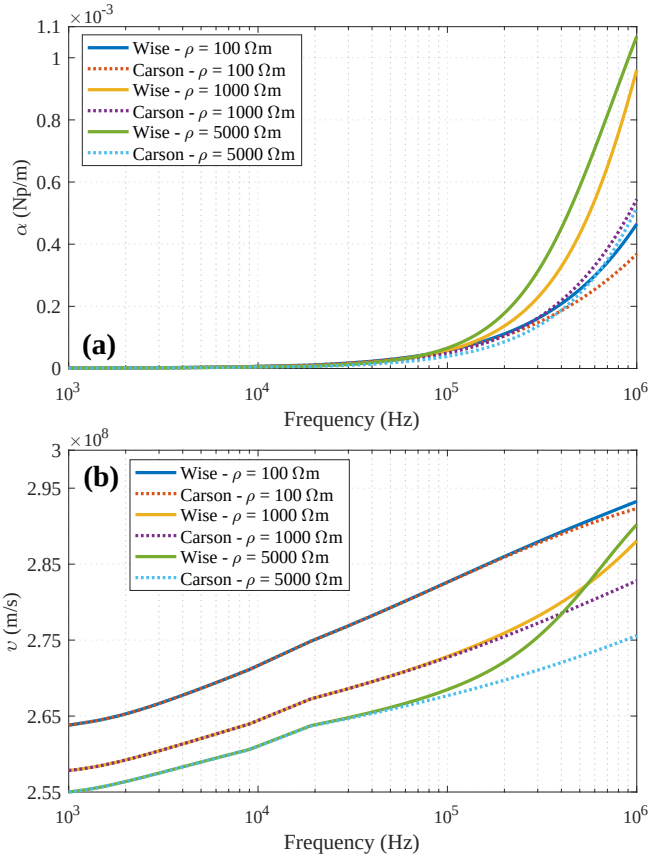

Fig. 8. Attenuation constant (a) and phase velocity (b) for mode #4 (pipeline mode), comparing Carson and Wise's admittance formulas, with constant soil properties and different soil resistivities.

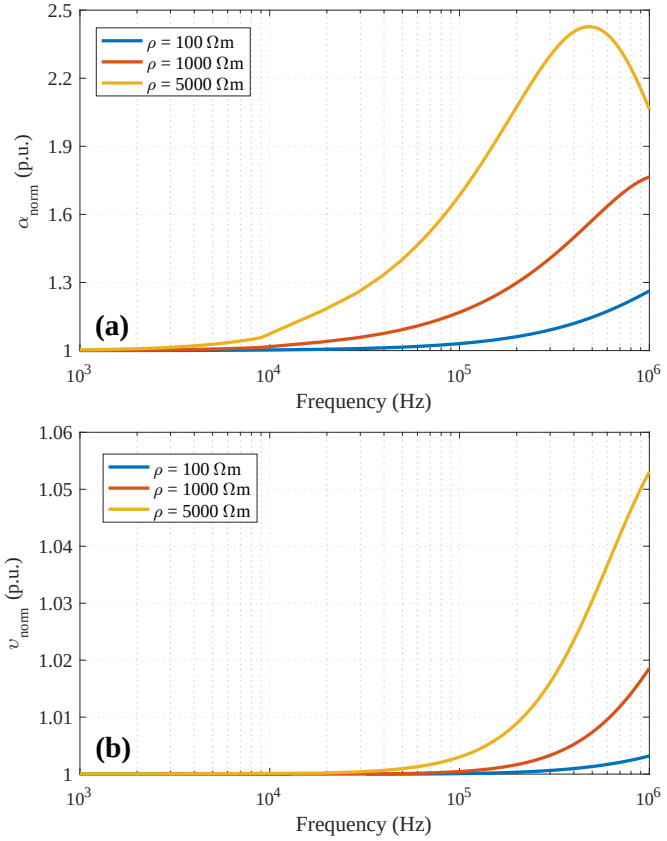

Fig. 9. Normalized attenuation constant (a) and phase velocity (b) for mode #4 (pipeline mode), comparing Carson and Wise's admittance formulas, with constant soil properties and different soil resistivities.

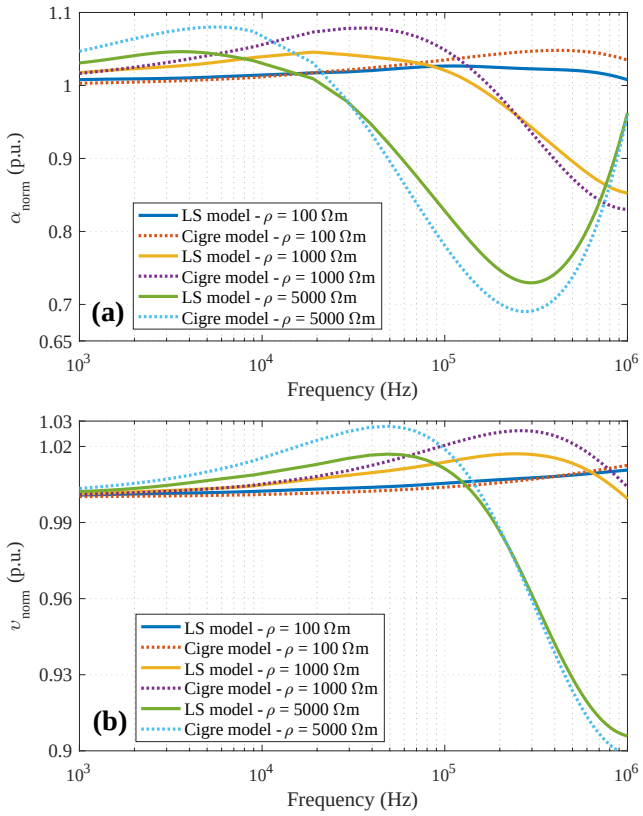

Fig. 10. Normalized attenuation constant (a) and phase velocity (b) for mode #3 (ground mode), comparing LS and CIGRE frequency-dependence models, using Wise's formula and different soil resistivities.

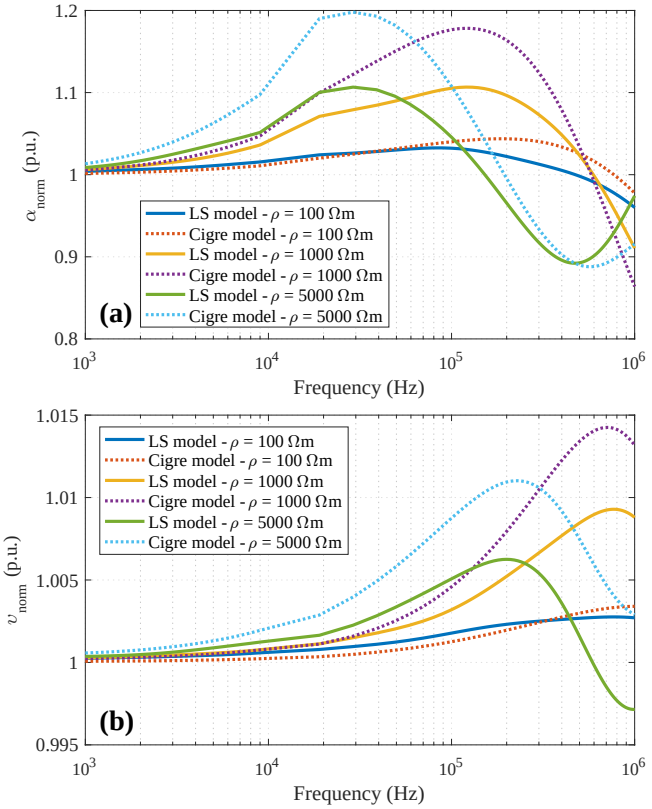

Fig. 11. Normalized attenuation constant (a) and phase velocity (b) for mode #4 (pipeline mode), comparing LS and CIGRE frequency-dependence models, using Wise's formula and different soil resistivities.